ISSN 0022-3727

Journal of Physics D
Applied Physics

Volume 42 Number 18 21 September 2009

Topical review

Model-based SEM for dimensional metrology tasks in semiconductor and mask industry

C G Frase, D Gnieser and H Bosse

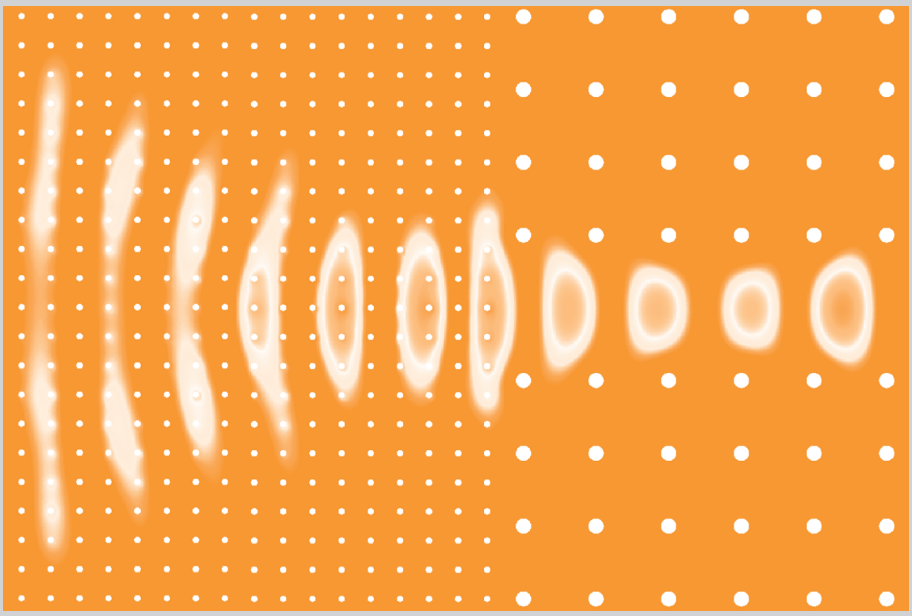

www.iop.org/journals/jphysd

IOP Publishing

IOP PUBLISHING JOURNAL OF PHYSICS D: APPLIED PHYSICS

J. Phys. D: Appl. Phys. **42** (2009) 185502 (5pp) doi:10.1088/0022-3727/42/18/185502

Acoustic beamwidth compressor using gradient-index phononic crystals

Sz-Chin Steven Lin[1], Bernhard R Tittmann[1], Jia-Hong Sun[2], Tsung-Tsong Wu[2] and Tony Jun Huang[1,3]

[1] Department of Engineering Science and Mechanics, The Pennsylvania State University, University Park, PA 16802, USA

[2] Institute of Applied Mechanics, National Taiwan University, Taipei 106, Taiwan

E-mail: junhuang@psu.edu

Received 29 May 2009, in final form 1 June 2009
Published 28 August 2009
Online at stacks.iop.org/JPhysD/42/185502

Abstract

We report a novel approach to effectively couple acoustic energy into a two-dimensional phononic-crystal waveguide by an acoustic beamwidth compressor using the concept of a gradient-index phononic crystal (GRIN PC). The GRIN PC-based beamwidth compressor is composed of a square array of solid scatterers embedded in epoxy. By gradually modulating the density and elastic modulus of the scatterers along the direction transverse to the phononic propagation, the beamwidth compressor can efficiently compress the wide acoustic beam to the scale of the phononic-crystal waveguide. This acoustic beamwidth compressor is investigated through a finite-difference time-domain method. A beam-size conversion ratio of 6.5 : 1 and a transmission efficiency of up to 90% is obtained over the working frequency range of the phononic-crystal waveguide. Potential applications for this device include acoustic biosensors and signal processors.

(Some figures in this article are in colour only in the electronic version)

Over the past decade, phononic crystals composed of a periodic array of elastic scatterers embedded in a host material have attracted a great deal of attention due to their ability to manipulate the propagation of acoustic waves on the wavelength scale [1, 2]. These engineered structures typically exhibit complete phononic bandgaps in their transmission spectra where mechanical vibrations in any polarization are suppressed and the propagation of acoustic waves is forbidden [3–11]. Phononic bandgaps result from destructive interference of reflections from the periodic scatterers. And their width and location can be adjusted by varying constitutive parameters (e.g. geometry, composition or material properties) of the structure, making phononic crystals promising structures as perfect acoustic mirrors and acoustic filters of designated frequencies [12, 13]. In addition, any defect inside a phononic crystal will limit acoustic waves to propagate only within the defect, making them useful as acoustic waveguides [14–19].

In the past years, researchers have developed phononic crystal-based waveguides that can efficiently guide acoustic waves along predefined pathways and sharp corners in a compact space on the order of several wavelengths down to the nanometre scale [14, 15]. Recently, several groups have studied the guiding of acoustic waves in straight- or bent-line phononic-crystal waveguides theoretically and experimentally [13, 16–19]. The width of a phononic-crystal waveguide is normally as narrow as one period of the crystal, allowing for wave propagation up to the gigahertz range, which can prove useful in micro/nanoscale acoustic circuits. However, the dimension mismatch between the input acoustic beam and the phononic-crystal waveguide could cause a great deal of energy loss, which is undesirable for practical applications. To fully realize the functionalities of a phononic-crystal waveguide, it is necessary to effectively couple acoustic energy into the waveguide over its working bandwidth. Traditional acoustic lenses that focus acoustic waves through curved surfaces are prone to misalignment and difficult fabrication. While phononic crystal-based flat lenses using negative refraction could be conveniently integrated with phononic-crystal waveguides, they are limited by their narrow working band and low gain [20, 21].

[3] Author to whom any correspondence should be addressed.

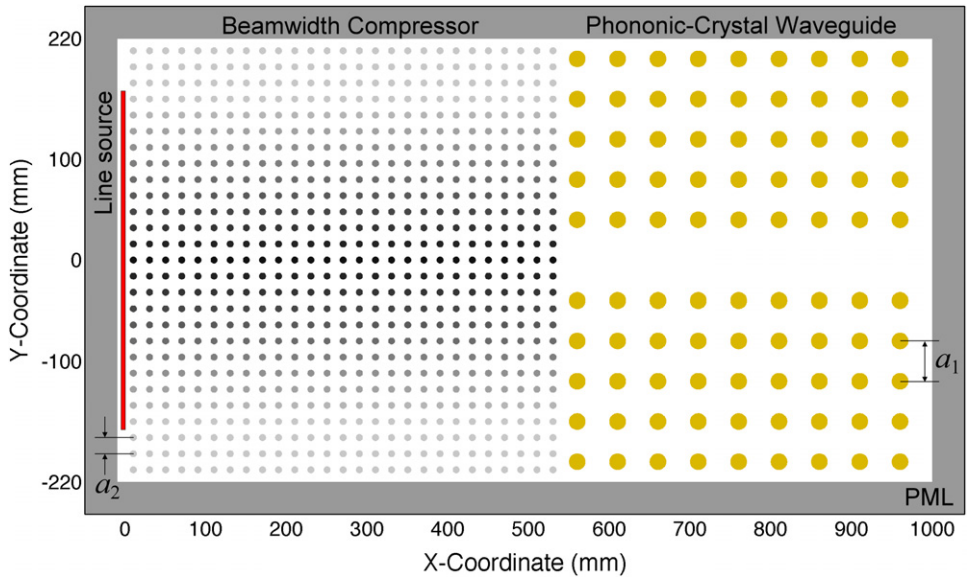

Figure 1. Schematic representation of the acoustic coupler design composed of a GRIN PC-based beamwidth compressor and a line-defect phononic-crystal waveguide. Different colour intensities represent different cylinder materials that are listed in table 1. A line source is placed in front of the beamwidth compressor to excite SV-mode BAW.

To achieve efficient acoustic beamwidth compression, we propose a novel approach to concentrate acoustic waves by employing a recently presented concept called gradient-index phononic crystals (GRIN PCs) [22]. We prove that using this approach, a wide acoustic beam can be efficiently coupled into a narrow phononic-crystal waveguide over a working bandwidth. This technique should be welcomed in applications where acoustic beamwidth compressors are needed to focus input and reference waves into a waveguide for nonlinear convolution processes [23].

The schematic illustration of the phononic crystal-based acoustic coupler is presented in figure 1. Although a phononic crystal supports propagation of multiple acoustic modes, in this paper we focus our investigation on the shear-vertical (SV) mode bulk acoustic wave (BAW). As shown in figure 1, a 336 mm wide line source is placed at $x = 0$ and polarized along the z coordinate to generate a SV-mode BAW with a uniform-amplitude distribution across the y coordinate. A GRIN PC-based beamwidth compressor is introduced next to the line source to compress wide-beam plane waves to a focal spot at the inlet of a straight phononic-crystal waveguide, guiding the coupled acoustic energy towards the outlet along the predefined path.

The phononic-crystal waveguide is obtained by simply removing the centre row of cylinders along the wave propagation direction (ΓX orientation in the wave-vector space) from a square-lattice phononic crystal composed of gold cylinders embedded in epoxy, as shown in figure 1. The lattice period (a_1) and the gold cylinder radius (r_1) were 40 mm and 4 mm, respectively. The width of the phononic-crystal waveguide, defined as the distance between adjacent cylinders on both sides of the waveguide, is 72 mm and its length is nine periods or 360 mm. For this arrangement, the gold/epoxy phononic crystal exhibits a bandgap for the SV-mode BAW from 10.88 (M_1) to 15.12 (X_2) KHz. Figure 2(a) shows the calculated dispersion curves via a finite-difference time-domain (FDTD) method without considering the thermal effects on material properties [14, 24, 25]. In order to understand the guided modes associated with the straight phononic-crystal waveguide, we calculated the dispersion curves of the waveguide by defining a super-cell of 11 periods in the y coordinate in the FDTD calculation [14]. In figure 2(b), the bandgap for the perfect gold/epoxy phononic crystal is delineated by two shaded regions. A narrow guided-mode bandgap for the SV-BAW was observed from 14.88 to 15.12 KHz. Hence, the phononic-crystal waveguide can operate continuously over the frequency from 10.88 to 14.88 KHz.

A GRIN PC [22] is an acoustic analogue of a gradient-index optical medium, where converging of propagating light is caused by a parabolic refractive-index gradient across the medium [26–29]. By gradually modulating the constitutive parameters (such as material properties and filling ratio) of a GRIN PC, one can induce an acoustic velocity variation along the modulating direction. Since the acoustic velocity in each row may vary for different propagating modes, GRIN PCs will have optimized performance for the designed acoustic mode. Based on this concept, the beamwidth compressor used in this work contains a 27 × 27 square array of solid cylinders embedded in epoxy. The lattice period (a_2) and the cylinder radius (r_2) were 16 mm and 1.6 mm, respectively. As shown in the schematic drawing in figure 1, 11 different solids were chosen to construct a parabolic acoustic velocity gradient along the y coordinate in the beamwidth compressor for the SV-mode BAW. The elastic properties of the chosen solids are listed in table 1. The dispersion curves of each row of the beamwidth compressor are plotted in figure 2(a). An enlargement at the design frequency of 13.66 KHz is shown in the inset of figure 2(a), from where the acoustic velocity in each row was determined from the relation: $v_g = \partial\omega/\partial k$, when

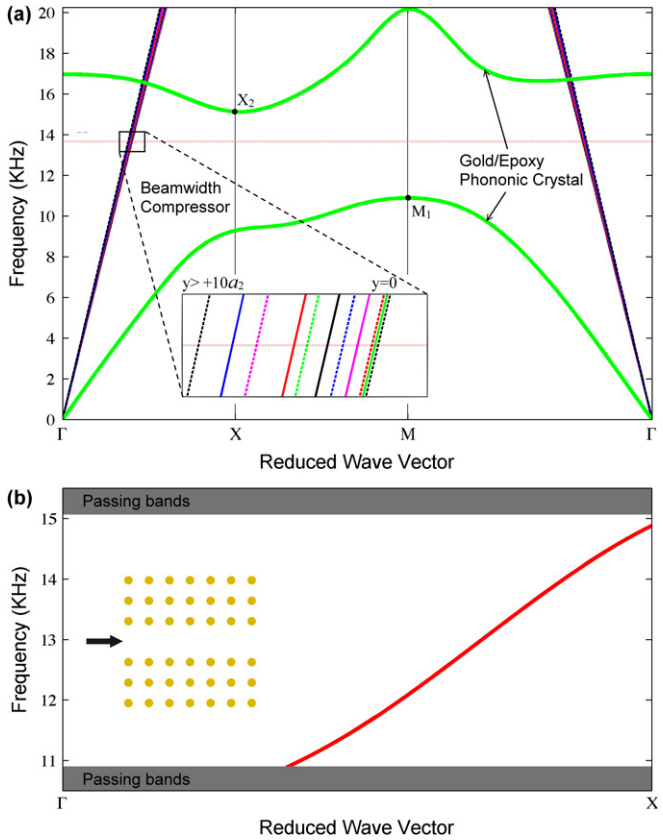

Figure 2. (*a*) The dispersion curves of the perfect gold/epoxy phononic crystal and each row of the GRIN PC-based beamwidth compressor for the SV-mode BAW. The notations Γ, M and X are the symmetry points of the first Brillouin zone in the wave-vector space. A parabolic gradient of acoustic velocity along the y coordinate in the beamwidth compressor was optimized at 13.66 KHz (dotted horizontal line) to compress incident waves to the inlet of the phononic-crystal waveguide. (*b*) The dispersion curves of the guided modes of the phononic-crystal waveguide.

ω represents angular velocity and k represents the wave vector. Note that within the working frequency of the phononic-crystal waveguide (10.88-14.88 KHz), the dispersion curves of all rows are nearly straight lines and thus the frequency-sensitivity of acoustic velocities is negligible. This fact suggests that though optimized at 13.66 KHz, the beamwidth compressor is not frequency-dispersive and can focus acoustic waves over the frequency range in a stable manner.

The length of the beamwidth compressor used in the acoustic coupler design was determined from studying the propagation of acoustic waves in an independent GRIN PC. A GRIN PC with a length of 960 mm (60 periods) surrounded by perfect matching layers (PMLs) at the boundaries was studied using a FDTD method [14, 30]. The FDTD program was developed from the theory of elasticity: the equation of motion and the constitutive law were discretized to simulate wave propagation in linear elastic materials. Figure 3 displays the simulated propagation of SV-BAWs excited at 13.66 KHz by a line source as described in figure 1. The amplitudes of displacement fields are shown in decibels (dB) and the colour distribution was normalized to the maximum value of the displacement. From figure 3, wide-beam plane waves bend gradually towards $y = 0$ where acoustic velocity was lowest per Snell's law and converged at a focal zone centred at $x = 480$ mm (30 periods) due to the gradient. Beyond that zone, the focused beams were redirected parallel to the direction of propagation and reform planar wavefronts at $x = 960$ mm. It can be seen that the peak acoustic intensity at the focal zone is 8 dB stronger than the input acoustic beam. The FWHM of the focused beam is 81 mm, equivalent to one wavelength of SV wave in epoxy ($\lambda = 83.3$ mm at 13.66 KHz). Since a beamwidth compressor of 27 periods (432 mm) is long enough for effective focusing, this length (432 mm) was used in the design of the acoustic coupler.

The simulated SV-BAW propagation in the proposed phononic crystal-based acoustic coupler at 13.66 KHz is shown in figure 4. It can be seen that wide-beam acoustic waves were well compressed by the beamwidth compressor and coupled into the phononic-crystal waveguide. To quantitatively analyse the effectiveness of the proposed beamwidth compressor, the steady-state transmitted acoustic energy was calculated at the outlet of the phononic-crystal waveguide. Since half of the acoustic energy generated by the line source propagates in the negative x direction, an intrinsic loss of -3 dB was included in the calculation of the transmission. The transmission spectra shown in figure 5(*a*) displays the transmissions of the acoustic coupler and a stand-alone phononic-crystal waveguide where the same acoustic waves were directly fed into the structure. The transmission in both cases drops noticeably as frequency approaches the guided-mode bandgap of the phononic-crystal waveguide. The stand-alone phononic-crystal waveguide exhibits a maximum transmission of -12.05 dB at 13.45 KHz, corresponding to a transmission rate of 12.5% (only considering acoustic energy propagating towards the positive x direction). By comparison, the proposed acoustic coupler exhibits an average transmission of -3.85 dB over a broad range of frequencies from 10.88 to 14.50 KHz corresponding to a transmission rate of 82.5%. A transmission rate up to 90% was obtained at frequencies close to the design frequency of the beamwidth compressor. Thus, the beamwidth compressor contributes to a transmission enhancement of 7.2 times.

Figure 5(*b*) plots the transverse displacement profiles of the input and guided beams at the entrance of the beamwidth compressor and the outlet of the phononic-crystal waveguide at 13.66 KHz. The profiles were normalized to the maximum amplitude of the guided beam. The input and guided beam have a FWHM of 336 mm and 51.5 mm, respectively. A beam-size conversion ratio of 6.5 : 1 was obtained in this work. While a reduction in the width of the phononic-crystal waveguide can increase the conversion ratio, the inlet of the phononic-crystal waveguide will need to be optimized to maintain good transmission. By increasing the number of rows in the beamwidth compressor and designing a smoother acoustic velocity gradient, wider acoustic beams can be compressed into the focal zone, increasing the conversion ratio without losing transmission efficiency.

Table 1. Elastic properties of the materials used in the beamwidth compressor and phononic-crystal waveguide.

Material	Density ($g\,cm^{-3}$)	V_L ($km\,s^{-1}$)	V_S ($km\,s^{-1}$)	y coordinate in beamwidth compressor
Epoxy	1.14	2.55	1.14	—
Gold	19.3	3.20	1.20	—
Copper	8.96	4.66	2.24	0
Bronze	8.86	3.53	2.23	$\pm a_2$
Niobium	8.57	4.92	2.10	$\pm 2a_2$
Titanium carbide	10.15	6.70	4.00	$\pm 3a_2$
Nickel	8.84	5.70	2.96	$\pm 4a_2$
Cast iron	7.70	5.90	2.40	$\pm 5a_2$
Zinc	7.10	4.20	2.41	$\pm 6a_2$
Zirconium	6.48	4.65	2.25	$\pm 7a_2$
Vanadium	6.03	6.00	2.78	$\pm 8a_2$
Nylon	1.12	2.60	1.10	$\pm 9a_2$
Titanium	4.54	6.10	3.12	$\geqslant \pm 10a_2$

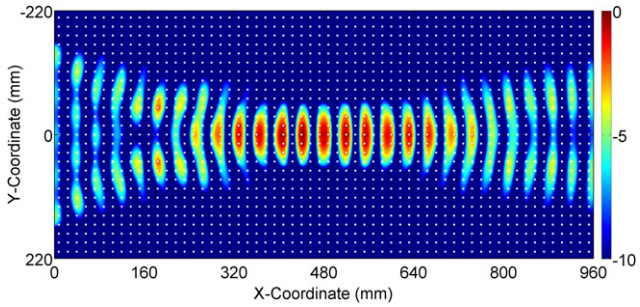

Figure 3. FDTD simulated acoustic wave propagation in a GRIN PC of length 960 mm (60 periods) at the design frequency of 13.66 KHz. The amplitudes of displacement fields are shown in decibels (dB).

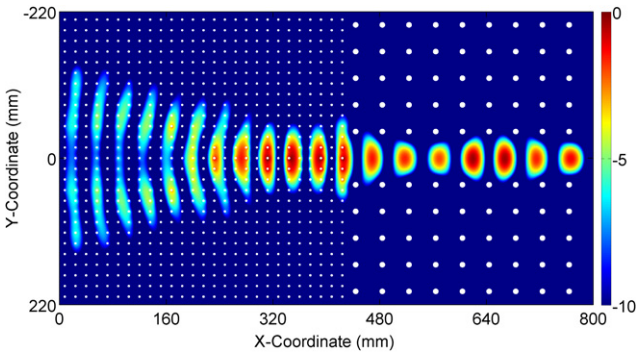

Figure 4. FDTD simulated acoustic wave propagation in the acoustic coupler at 13.66 KHz. Displacement fields were normalized to the maximum displacement of the guided beam.

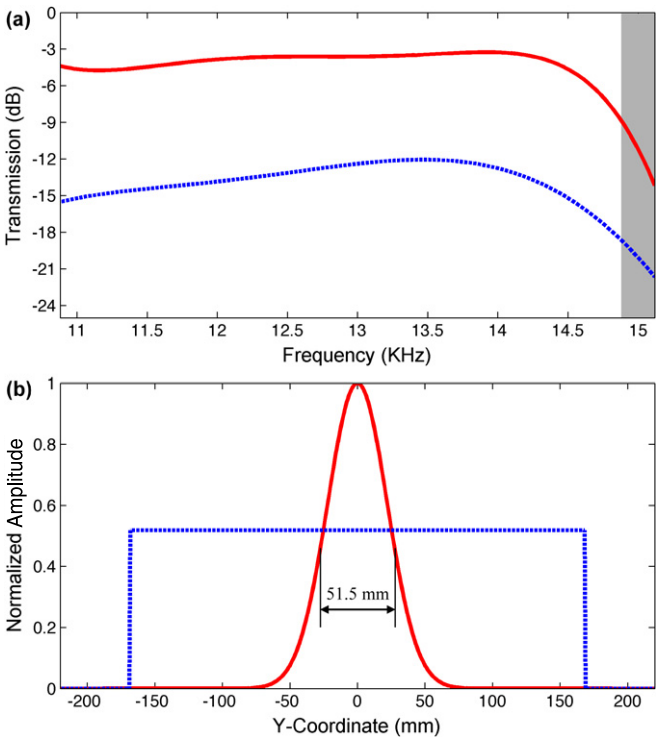

Figure 5. (*a*) Transmission for the acoustic coupler (solid line) and a stand-alone phononic-crystal waveguide (dashed line). The shaded region denotes the guided-mode bandgap of the phononic-crystal waveguide. (*b*) The transverse displacement profiles of acoustic waves at the entrance of the beamwidth compressor (dashed line) and the outlet of the phononic-crystal waveguide (solid line) at 13.66 KHz.

In conclusion, we demonstrate a beamwidth compressor using the concept of GRIN PC to couple acoustic waves into a phononic-crystal waveguide. The GRIN PC-based beamwidth compressor exhibits a beam-size conversion ratio of 6.5 : 1 and a transmission efficiency of up to 90% over the working frequency range of a straight phononic-crystal waveguide. A transmission enhancement of 7.2 times was obtained compared with a stand-alone phononic-crystal waveguide. The acoustic beamwidth compressor is compact and flat, and it operates stably over a wide frequency range. Due to these advantages, the methodology described in this work can be useful in many applications relating to signal processors [23], acoustic sensors [31] and cell patterning [32].

Acknowledgments

The authors thank Aitan Lawit for the helpful discussions. They also acknowledge support from the High Performance Computing Group at the Pennsylvania State University. This research was supported by the National Science Foundation (ECCS-0824183 and ECCS-0801922) and the Penn State Center for Nanoscale Science (MRSEC).

References

[1] Yablonovitch E 1987 *Phys. Rev. Lett.* **58** 2059
[2] Kushwaha M S, Halevi P, Dobrzynski L and Djafari-Rouhani B 1993 *Phys. Rev. Lett.* **71** 2022
[3] Vines R E, Wolfe J P and Every A V 1999 *Phys. Rev.* B **60** 11871
[4] Psarobas I E, Stefanou N and Modinos A 2000 *Phys. Rev.* B **62** 278
[5] Cervera F, Sanchis L, Sánchez-Pérez J V, Martínez-Sala R, Rubio C, Meseguer F, López C, Caballero D and Sánchez-Dehesa J 2001 *Phys. Rev. Lett.* **88** 023902
[6] Ruzzene M, Scarpa F and Soranna F 2003 *Smart Mater. Struct.* **12** 363
[7] Wu T T, Huang Z G and Lin S 2004 *Phys. Rev.* B **69** 094301
[8] Yan Z Z and Wang Y 2006 *Phys. Rev.* B **74** 224303
[9] Sutter-Widmer D, Deloudi S and Steurer W 2007 *Phys. Rev.* B **75** 094304
[10] Shi J, Lin S C S and Huang T J 2008 *Appl. Phys. Lett.* **92** 111901
[11] Hou Z and Assouar B M 2008 *Phys. Lett.* A **372** 2091
[12] Sigalas M M 1998 *J. Appl. Phys.* **84** 3026
[13] Bria D and Djafari-Rouhani B 2002 *Phys. Rev.* E **66** 056609
[14] Sun J H and Wu T T 2006 *Phys. Rev.* B **74** 174305
[15] Lin K H, Chang C F, Pan C C, Chyi J I, Keller S, Mishra U, DenBaars S P and Sun C K 2006 *Appl. Phys. Lett.* **89** 143103
[16] Khelif A, Choujaa A, Benchabane S, Djafari-Rouhani B and Laude V 2004 *Appl. Phys. Lett.* **84** 4400
[17] Yao Y W, Hou Z L and Liu Y Y 2006 *J. Phys. D: Appl. Phys.* **39** 5164
[18] Tanaka Y, Yano T and Tamura S I 2007 *Wave Motion* **44** 501
[19] Olsson R H III and El-Kady I 2009 *Meas. Sci. Technol.* **20** 012002
[20] Yang S, Page J H, Liu Z, Cowan M L, Chan C T and Sheng P 2004 *Phys. Rev. Lett.* **93** 024301
[21] Zhang X and Liu Z 2004 *Appl. Phys. Lett.* **85** 341
[22] Lin S C S, Huang T J, Sun J H and Wu T T 2009 *Phys. Rev.* B **79** 094302
[23] Campbell C K 1998 *Surface Acoustic Wave Devices for Mobile and Wireless Communications* (San Diego, CA: Academic)
[24] Hsieh P F, Wu T T and Sun J H 2006 *IEEE Trans. Ultrason., Ferroelect., Freq. Control* **53** 148
[25] Yang R and Chen G 2006 *Phys. Rev.* B **69** 195316
[26] Gómez-Reino C, Perez M V and Bao C 2002 *Gradient-index Optics: Fundamentals and Applications* (Berlin: Springer)
[27] Centeno E, Cassagne D and Albert J P 2006 *Phys. Rev.* B **73** 235119
[28] Juluri B K, Lin S C S, Walker T R, Jensen L and Huang T J 2009 *Opt. Express* **17** 2997
[29] Mao X, Lin S C S, Lapsley M I, Shi J, Juluri B K and Huang T J 2009 *Lab Chip* **9** 2050
[30] Berenger J 1994 *J. Comput. Phys.* **114** 185
[31] Lucklum R and Hauptmann P 2006 *Anal. Bioanal. Chem.* **384** 667
[32] Shi J, Mao X, Ahmed D, Colletti A and Huang T J 2008 *Lab Chip* **8** 221